INTERNATIONAL JOURNAL OF RESEARCH
In Advanced Engineering Technologies

Volume 6, Issue 2 OCT 2017

DESIGN AND ANALYSIS OF SYNCHRONOUS WIND POWER GENERATORS WITH MAXIMUM POWER TRACKING SCHEME

[1]NALADIMMU RAJASEKHAR REDDY, [2]CH.RAMI REDDY
[1]M.Tech, NALANDA INSTITUTE OF ENGINEERING & TECHNOLOGY
[2]Assistant Professor, NALANDA INSTITUTE OF ENGINEERING & TECHNOLOGY

ABSTRACT-This paper presented an excitation synchronous wind power generator with MPTC scheme. A novel excitation synchronous wind power generator (ESWPG) with a maximum power tracking scheme is proposed in this paper. The servo motor provides controllable power to regulate the rotor speed and voltage phase under wind disturbance. The excitation synchronous generator and servo motor rotor speed tracks the grid frequency and phase using the proposed coaxial configuration and phase tracking technologies. The wind and servo motor powers are integrated with each other and transmitted to the excitation synchronous generator via a coaxial configuration. The generator output can thus be directly connected to the grid network without an additional power converter. The proposed maximum power tracking scheme governs the exciter current to achieve stable voltage, maximum power tracking, and diminishing servo motor power consumption. The system transient and static responses over a wide range of input wind power are examined using simulated software.

Index Terms—Excitation synchronous generator, maximum power tracking, servo motor control, wind power

I.INTRODUCTION

This paper presents a novel converter less wind power generator with a control framework that consists of an excitation synchronous generator, permanent magnet (PM) synchronous servo motor, signal sensors, and servo control system. Wind power generators can be divided into induction and synchronous types [1]–[4]. The excitation synchronous generator driven by hydraulic, steam turbine, or diesel engines has been extensively adopted in large-scale utility power generation owing to desired features such as high efficiency, reliability, and controllable output power. A wind power generator in grid connection applications, except for doubly fed induction generators, achieves these features using variable speed constant frequency technology. However, most excitation synchronous wind generators cannot be connected directly to the grid, owing to instabilities in wind power dynamics and unpredictable properties that influence the generator synchronous speed.

The direct drive permanent magnet synchronous wind generator (PMSWG) uses variable speed and power converter technologies to fulfill the grid connection requirements, which has advantages of being gearless. Various power transfer technologies are applied for ac/dc transformation to obtain a constant frequency ac power [4]–[6]. However, extensive use of power electronic devices in those systems that will cause unavoidable power losses from the rectifier's conducting resistance and high-frequency power switches, which will increase power consumption. Therefore, a converter less method for a high-efficiency excitation synchronous wind generator is an important issue, especially for middle and high output voltage wind power generators.

The wind and servo motor powers are integrated with each other and transmitted to the excitation synchronous generator via a coaxial configuration. When the wind speed varies, the servo motor provides a compensatory energy to maintain constant generator speed. According to the servo motor power magnitude and the generator power, the proposed maximum power tracking scheme controls the excitation field current to ensure that the excitation synchronous generator fully absorbs the wind power, and converts it into electricity for the loads.

II. POWERFLOW ANDSPEED

For simplicity, assume that all energy transmission elements behave ideally, allowing us to ignore the mechanical power losses of the wind turbine, the servo motor, and the excitation synchronous generator.

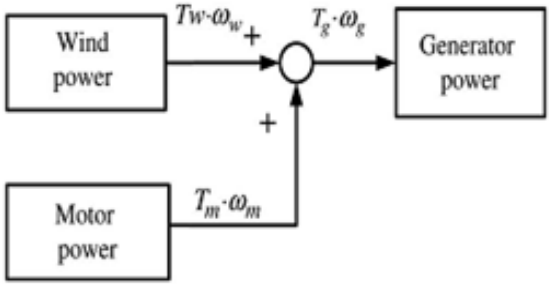

Fig. 1.Power flow block diagram.

Fig. 1 shows the power flows of the proposed system, where T_w $T_{m,}$, and $T_g$denote the

torques and ω_w ,$\omega_m$and ω_g are the wind turbine, servo motor, and excitation synchronous generator speeds, respectively. The total excitation synchronous generator input power is the product of T_g and ω_g. The power flow equation can thus be defined as

$$T_g.w_g = T_w.w_w + T_m w_m \quad (1)$$

Fig. 2 shows the corresponding coaxial configuration. The wind generator rotor shaft input-end receives rotating torques from the speed increasing gear box.

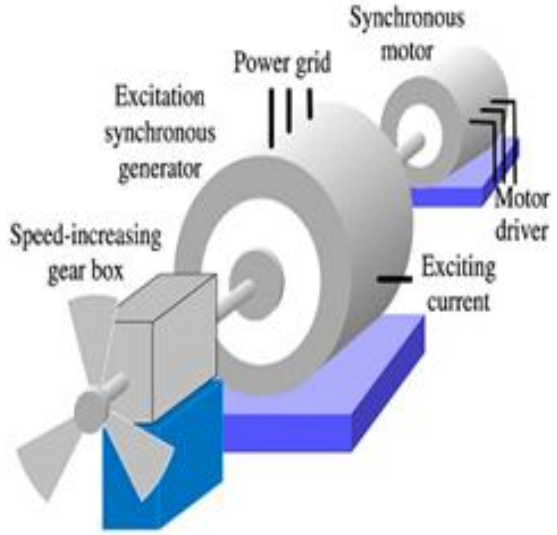

Fig. 2. Proposed coaxial construction configuration

The tail-end of the generator rotor shaft is coupled with a servo motor. The input energy of the excitation synchronous generator is the sum of the wind power and servo motor powers. The speed and rotating direction for the wind turbine output, servo motor, and excitation synchronous generator is the same, i.e., the system speeds satisfy $\omega_w = \omega_m = \omega_g$,. This arrangement can reduce the power transmission losses.

III. CONTROLPRINCIPLES OFPROPOSEDWIND POWER GENERATORSYSTEM

Fig. 3 depicts the control framework of the proposed system. The control system design concepts maintain power flow balance between the input and the output and, simultaneously, force the generator frequency to synchronize with the utility grid. When the system complies with these conditions, the generator output can be connected to the utility grid network, subsequently reaching the high efficiency and maximum power tracking objectives. The control signals, including the generator voltage, current, grid phase, motor encoder, and output power, are sensed and transferred to the microprocessor control unit (MCU).

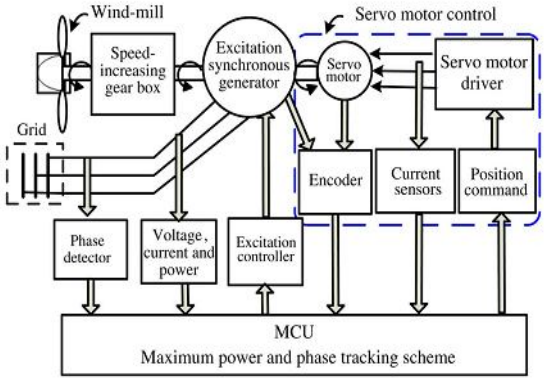

Fig. 3. Proposed wind power system framework.

The servo motor controller plays an important role in output power and grid voltage phase tracking. A chain reaction subsequently occurs in which the servo motor power returns to a balanced level. During the energy balance periods, the servo motor consumes only a slight amount of energy to stabilize the shaft speed.

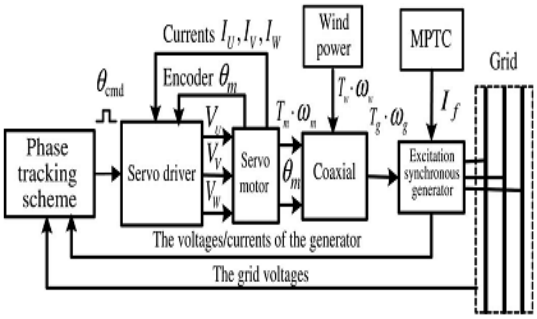

Fig. 4. Proposed wind power generator system

Fig. 4 schematically depicts the servo motor and maximum power tracking control (MPTC) loops which are designed to stabilize the speed, frequency, and output power of the excitation synchronous generator under wind disturbances. The phase/frequency synchronization strategy in Fig. 4 compares the grid voltage-phase and frequency with the generator's feedback signals, and produces the position command θ_{cmd} with pulse-type signals to the servo motor driver.

The MPTC also adjusts the excitation field current I_f based on the wind power and motor power inputs, where θ_m denotes the servo motor rotor mechanical rotor angular displacement detected by an encoder. Due to the coaxial configuration, detecting the relative position of the rotor allows us to determine the generator voltage phase during the wind power generator system operating in the grid connection state.

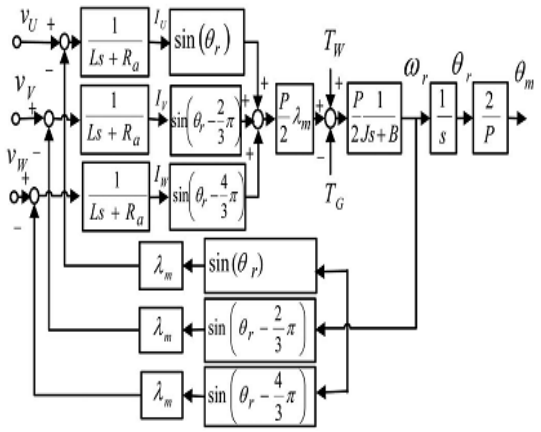

Fig. 5. PM synchronous motor block diagram.

TABLE I
PARAMETERS OFPM
SYNCHRONOUSMOTOR

Item	Value
Flux linkage of stator winding (λ_m)	0.27 Vs / rad
PWM constant gain (K_a)	10
Rotor inertia (J)	3.3×10^{-4} kg·m^2
Viscous-friction coefficient (B)	0.0 Nm/s
Stator wining resistance (R_a)	1.5 Ω
Stator wining inductance (L)	8 mH
Motor poles (P)	8-pole

IV. SERVOMOTORCONTROLLERDESIGN

The transient and dynamic responses of the servo motor controller must satisfy robustness requirements to reduce the influence of windfluctuations to the generator. Thus, the robust integral structure control (RISC) method is chosen to ensure the voltage phase and the frequency in phase with the grid. Fig. 5 shows the block diagram of the three-phase PM synchronous motor, and Table I lists the parameters of the PM synchronous motor. According to (1), wind power, generator power, and servo motor power can be transformed into three torque functions and incorporated in the three-phase PM synchronous motor model. The electromagnetic torque of the servo motor can be expressed as [17]

$$T_m = \frac{P}{2} L_m \cdot \left[I_{v.} \sin\theta_r + I_{v.} \sin\left(\theta_r - \frac{2}{3}\pi\right) + I_w \cdot \sin\theta_r - \frac{4}{3}\pi \right] (2)$$

Where P denotes the number of motor poles, and I_U, I_V, and I_W are the applied stator currents. The mechanical torque can be expressed as

$$T_m + \left(T_m - T_q\right) = J_s \left(\frac{2}{P}\right) \frac{d_{w_r}}{dt} + B \left(\frac{2}{P}\right) w_r$$

$$\theta_r = \int w_r dt$$

$$\theta_r = \frac{2}{P} \theta_r (3)$$

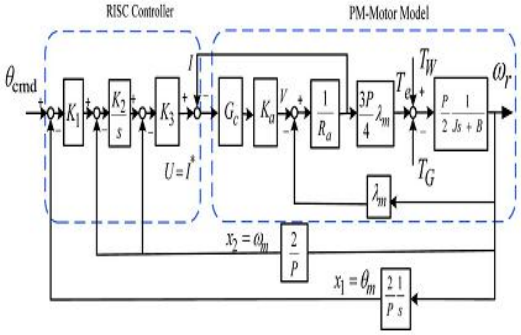

Fig. 6. Servo motor position control loops.

Additionally, denotes the electrical rotor angular velocity; represents the electrical rotor angular displacement; is the mechanical rotor angular displacement; is the rotor inertia; and is the damping coefficient.

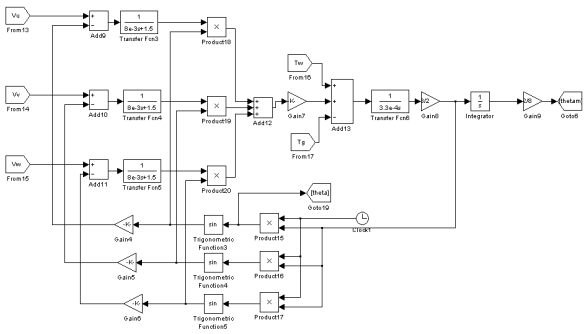

Fig. 5. PM synchronous motor block diagram

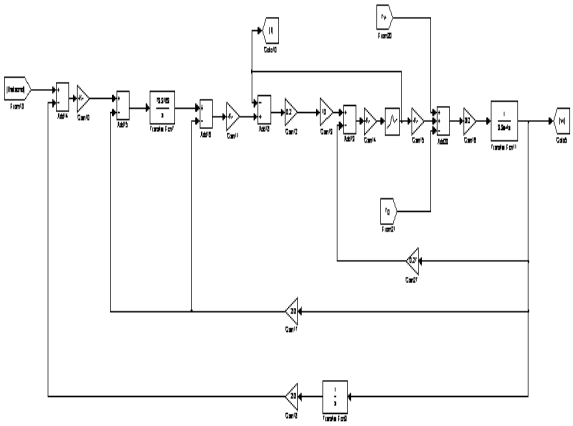

Fig. 6. Servo motor position control loops

Additionally ωr, denotes the electrical rotor angular velocity;θr represents the electrical rotor angular displacement θm; is the mechanical rotor angular displacement; J is the rotor inertia; and B is the damping coefficient. In Fig. 5, L denotes the inductance of the stator windings; λm represents the amplitude of the flux linkage established by the permanent magnet as viewed from the stator windings; Uu,Uv, and Uw are the applied stator voltage of the motor; and Ra denotes the resistance of

each stator winding. According to Fig. 6, the position control structure includes the RISC and servo motor transfer function. The conventional motor current feedback controller can avoid instantaneous current stress to the servo driver. This technology has been applied to the servo motor control to improve the control performance. The RISC outer loop is designed to achieve a fast and accurate servo tracking response under load disturbances and plant parameter variations.In Fig. 6, θcmd denotes the position command. Parameters K1 and K3 are proportional gains and K2 is the integral gain. The PM synchronous motor state equations are described as

$$\begin{cases} x_1(t) = x_2(t) \\ x_2(t) = -a_1x_1(t) - a_2x_2(t) + bU(t) - T_L(t) \end{cases} \quad (4)$$

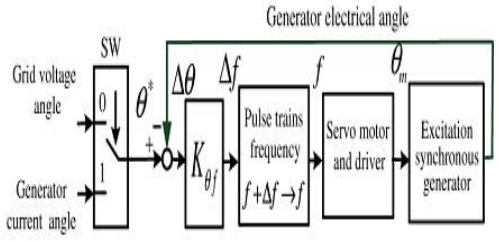

Fig. 7. Phase tracking control scheme.

Where x1 is θr and x2 is ωr

$$\begin{cases} a_1 = 0 \\ a_2 = \frac{B}{J} + \frac{\frac{3P}{4}\lambda_m{}^2}{JR_a + JG_cK_a} \\ b = \frac{\frac{3p}{4}GcK_a\lambda_m}{JR_a + JG_cK_a} \\ T_L = \frac{1}{J}(T_w - T_g) \end{cases} \quad (5)$$

RISC is a typical state feedback control scheme that combines an integral controller and the plant series state feedback information. TL refers to the total disturbance which is defined in (5), and U is the system control function. For a third RISC system, the control function U can be expressed as follows

$$U(s) = K_1K_2K_3\frac{\theta_{cmd} - x_1(s)}{s} - K_2K_3x_1 - K_3x_2 \quad (6)$$

Transfer function of the system is

$$\frac{x_1(s)}{\theta_{cmd}(s)} = \frac{K_1K_2K_3b}{s^3 + (a_2 + K_3b)s^2 + (a_1 + K_2K_3b)s + K_1K_2K_3b} \quad (7)$$

By designing the system characteristic function to lie on the stable plane, one can obtain

$$(s + \lambda_1)(s + \lambda_2)(s + \lambda_3) += 0 \quad (8)$$

where λ1,λ2, and λ3 are the system selected close-loop poles. The characteristic function of (7) can then be rewritten as

$$S^3 + (\lambda_1 + \lambda_2 + \lambda_3)S^2 + (\lambda_1\lambda_2 + \lambda_1\lambda_3 + \lambda_2\lambda_3)S + \lambda_1\lambda_2\lambda_3 = 0 \quad (9)$$

The system control gain K1 ,K2 , and K3 can be determined by (9) and the pole-zero placement method

$$\begin{cases} K_3 = \frac{(\lambda_1 + \lambda_2 + \lambda_3) - a_2}{b} \\ K_2 = \frac{(\lambda_1\lambda_2 + \lambda_2\lambda_3 + \lambda_1\lambda_3) - a_1}{K_3b} \\ K_1 = \frac{\lambda_1\lambda_2\lambda_3}{K_2K_3b} \end{cases} \quad (10)$$

PHASE TRACKING CONTROL SCHEME

Fig. 7 depicts the proposed phase tracking control scheme. Before the excitation synchronous generator system connects to the grid (SW=0),θ* equals to the grid voltage angle. With the coaxial configuration described in Section II, the servo motor and generator electrical angle can be obtained using the motor encoder and the grid voltage sensor, respectively. The MCU

compares the phase difference between the two signals, and gradually adjusts the excitation synchronous generator rotor position to reduce the phase deviation. Fig. 7 reveals that, while the proposed system contains a phase deviation Δθ, the deviation frequency Δf can be expressed as follows:

$$\Delta f = K_{\theta f} \times \Delta\theta \quad (11)$$

where Kθf denotes a constant gain. The new pulse frequency f can be obtained as follows:

$$f + \Delta f \rightarrow f \quad (12)$$

The MCU generates pulse trains of frequency command f for the servo motor to drive the servo motor, explaining why the generator can lock the generator frequency and phase in the phase command. When the generator is connected to the grid (SW=1) θ* equals the generator current angle. MCU calculates the generator electrical angle and current phase angle difference to adjust the generator rotor position to reduce the phase deviation. Consequently, the generator power factor can be controlled and improved.

MAXIMUM POWER TRACKING CONTROL

In a natural environment, the wind power varies with time. To stabilize the generator output voltage, current, and output power, the excitation synchronous generator output power has to track the input power variation and react immediately by adjusting the excitation field current. In this paper, a maximum power tracking control scheme is proposed. The proposed MPTC scheme includes two control loops as shown in Fig. 8, which is motor

power control loop, and the generator power control loop. By MPTC scheme, it can make the motor consumption power minimize and most of wind power can be transferred to the grid by the generator. The control strategy describes as follows. As shown in Fig. 8, (1) can be rewritten as

$$P_{g-in} = P_w(w_w) + P_m$$

THREE-PHASE EXCITATION SYNCHRONOUS GENERATOR MODEL

For a typical three phases, four poles excitation synchronous generator, the generator output power is governed by the excitation controller, through the slip rings, with the appropriate excitation current sent to the armature winding. Based on the rotating magnetic field affection, the stator windings induce three-phase alternate voltages which have frequency in synchronization with the rotor speed. According to the conductor's electromagnetism and the mechanical forces on the stator winding and rotor, the generator back electromotive force voltage can be defined as

$$E = l.w_g \times B$$

where denotes the back electromotive force voltage of the excitation synchronous generator stator; represents the conductance magnet effective length; is the rotor speed; and is the magnetic field strength. The magnetic field strength can also be rewritten as

$$B = \frac{\mu N}{l} I_f$$

where denotes the conductance magnet permeability coefficient represents the number of winding turns; and is the rotor current. Combining (14) and (15) yields

$$E = \mu N.W_g.I_f$$

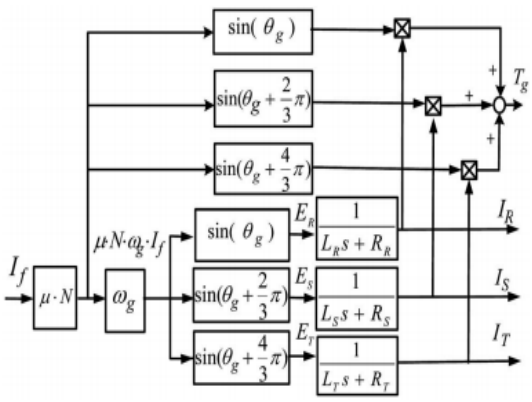

Fig. 9. Three-phase excitation synchronous generator

SIMULATION RESULTS

The generator design functionality is confirmed using a wind power generator framework simulation model with an excitation synchronous generator and its corresponding sub-systems. Tables I and II list the parameters of the PM synchronous motor, excitation synchronous generator.

TABLE II
PARAMETERS
OFEXCITATIONSYNCHRONOUSGENERATOR

Item	Value
Rated power output	3kW
Rated voltage output	AC 220V
Phase	3-phase
Pole	4-pole
Stator phase resistance (R_R , R_S , R_T)	0.17 Ω
Stator phase inductance (L_R , L_S , L_T)	4.3mH
Product of coefficient of conductance magnet and winding turn ($\mu \cdot N$)	0.04

TABLE III
GAINS OFPI CONTROLLER FORMPTC

Item	Value
Proportional gain (K_{p1})	1
Integral gain (K_{I1})	10
Proportional gain (K_{P2})	0.6
Integral gain (K_{I2})	10
Excitation gain (K_f)	0.2

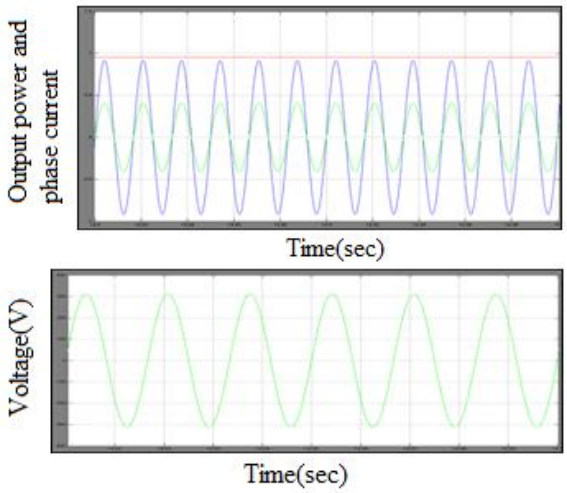

Fig. 10.Simulation results. (a) Phase voltage and current of the excitationsynchronous generator. (b) Voltage phase tracking

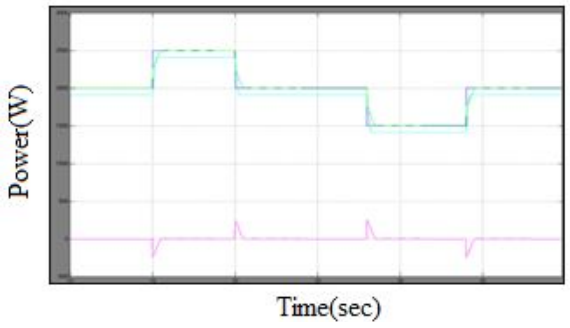

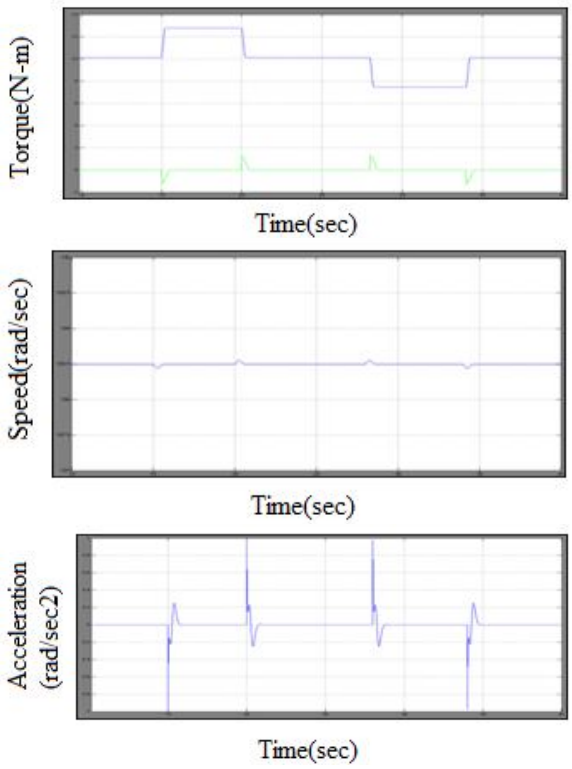

Fig. 11.Maximum power tracking simulation results. (a) Power tracking curves.(b) Generator input torque. (c) Shaft speed. (d) Shaft acceleration.

The voltage phase tracking performance of the system at generator output 2 kW is investigated. Fig. 10(a) shows the phase voltage and current wave forms of the excitation synchronous generator. Fig. 10(b) shows the grid and generator voltage phase tracking wave forms. The wind power generator system can thus connect directly to the grid. For evaluating the system performance under grid connection, input wind with step changes were applied.

CONCLUSION

An excitation synchronous wind power generator with MPTC scheme is proposed in this paper. The excitation synchronous generator andservo motor rotor speed tracks the grid frequency and phaseusing the proposed coaxial configuration and phase trackingtechnologiesIn the proposed framework, the servo motor provides controllable power to regulate the rotor speed and voltage phase under wind disturbance. Using a phase tracking control strategy, the proposed system can achieve smaller voltage phase deviations in the excitation synchronous generator. In addition, the maximum output power tracking scheme governs the input and output powers to achieve high performance. The excitation synchronous generator and control function models were designed from the physical perspective to examine the presented functions in the proposed framework. By using the simulation results we can analyze that the proposed wind power generator system achieves high performance power generation with salient power quality.The proposed maximum power tracking scheme governs the exciter current to achieve stable voltage,maximum power tracking, and diminishing servo motor power consumption.

REFERENCES

[1] M. Liserre, R. Cárdenas, M. Molinas, and J. Rodriguez, “Overview of Multi-MW wind turbines and wind parks,” IEEE Trans. Ind. Electron., vol. 58, no. 4, pp. 1081–1095, Apr. 2011.

[2] V. DelliColli, F. Marignetti, and C. Attaianese, “Analytical and multiphysics approach to the optimal design of a 10-MW DFIG for direct-drive wind turbines,” IEEE Trans. Ind. Electron., vol. 59, no. 7, pp. 2791–2799, Jul. 2012.

[3] B. Singh and S. Sharma, “Design and implementation of four-leg voltagesource-converter-based VFC for autonomous wind energy conversion system,” IEEE Trans. Ind. Electron., vol. 59, no. 12, pp. 4694–4703, Dec. 2012.

[4] A. Di Gerlando, G. Foglia, M. F. Iacchetti, and R. Perini, “Axial flux pm machines with concentrated armature windings: Design analysis and test validation of wind energy generators,” IEEE Trans. Ind. Electron., vol. 58, no. 9, pp. 3795–3805, Sep. 2011.

[5] S. Zhang, K.-J.Tseng, D. M. Vilathgamuwa, T. D. Nguyen, and X.-Y. Wang, “Design of a robust grid interface system for PMSG-based wind turbine generators,” IEEE Trans. Ind. Electron., vol. 58, no. 1, pp. 316–328, Jan. 2011.

[6] F. Bu, W. Huang, Y. Hu, and K. Shi, “An excitation-capacitor-optimized dual stator-winding induction generator with the static excitation controller for wind power application,” IEEE Trans. Energy Convers., vol. 26, no. 1, pp. 122–131, Mar. 2011.

[7] S. Le-peng, T. De-dong, W. Debiao, and L. Hui “Simulation for strategy of maximal wind energy capture of doubly fed induction generators,” in Proc. IEEE Int. Conf. Cognit.Informat., Jul. 2010, pp. 869–873.

[8] W. Qi, C. Xiao-hu, F. Wan-min, and J. Yan-chao, “Study of brushless doubly-fed control for VSCF wind power generation system connected to grid,” in Proc. Int. Conf. Electr. Utility Deregulation Restruct. Power Technol., Apr. 2008, pp. 2453–2458.

[9] A.Mesemanolis, C. Mademlis, and I. Kioskeridis, “Maximum efficiency of a wind energy conversion system with a PM synchronous generator,” in Proc. IEEE Int. Conf. Exhib. Power Gener.Transm.Distrib. Energy Convers, Ayia Napa, Cyprus, Nov. 2010, pp. 1–9.

[10] H. Geng, D. Xu, B. Wu, and G. Yang, "Active damping for PMSG-based WECS with DC-link current estimation," IEEE Trans. Ind. Electron., vol. 58, no. 4, pp. 1110–1119, Apr. 2011.
[11] W.-M.Lin and C.-M. Hong,"A new Elman neural network-based control algorithm for adjustable-pitch variable-speed wind-energy conversion systems," IEEE Trans. Power Electron., vol. 26, no. 2, pp. 473–481, Feb. 2011.
[12] C. Xia, Q. Geng, X. Gu, T. Shi, and Z. Song, "Input–output feedback linearization, and speed control of a surface permanent-magnet synchronous wind generator with the boost-chopper converter," IEEE Trans. Ind. Electron., vol. 59, no. 9, pp. 3489–3500, Sep. 2012.
[13] J. H. Zhao, F. Wen, Z. Y. Dong, Y. Xue, and K. P. Wong, "Optimal dispatch of electric vehicles, and wind power using enhanced particle swarm optimization," IEEE Trans. Ind. Inf., vol. 8, no. 4, pp. 889–899, Nov. 2012.